Oxygen isotope effects on lattice properties of $La_{2-x}Ba_xCuO_4$ ($x = 1/8$)

Z. Guguchia,[1,2,*] D. Sheptyakov,[3] E. Pomjakushina,[4] K. Conder,[4] R. Khasanov,[2] A. Shengelaya,[5] A. Simon,[6] A. Bussmann-Holder,[6] and H. Keller[1]

[1]*Physik-Institut der Universität Zürich, Winterthurerstrasse 190, CH-8057 Zürich, Switzerland*
[2]*Laboratory for Muon Spin Spectroscopy, Paul Scherrer Institut, CH-5232 Villigen PSI, Switzerland*
[3]*Laboratory for Neutron Scattering and Imaging, Paul Scherrer Institut, CH-5232 Villigen PSI, Switzerland*
[4]*Laboratory for Developments and Methods, Paul Scherrer Institut, CH-5232 Villigen PSI, Switzerland*
[5]*Department of Physics, Tbilisi State University, Chavchavadze 3, GE-0128 Tbilisi, Georgia*
[6]*Max Planck Institute for Solid State Research, Heisenbergstrasse 1, D-70569 Stuttgart, Germany*

(Received 18 March 2015; published 13 July 2015)

A negative oxygen-isotope ($^{16}O/^{18}O$) effect (OIE) on the low-temperature tetragonal (LTT) phase-transition temperature T_{LTT} was observed in $La_{2-x}Ba_xCuO_4$ ($x = 1/8$) using high-resolution neutron powder diffraction. The corresponding OIE exponent $\alpha_{T_{LTT}} = -0.36(5)$ has the same sign as $\alpha_{T_{so}} = -0.57(6)$ found for the spin-stripe order temperature T_{so}. The fact that the LTT transition is accompanied by charge ordering (CO) implies the presence of an OIE also for the CO temperature T_{co}. Furthermore, a temperature-dependent shortening of the c axis with the heavier isotope is observed. These results combined with model calculations demonstrate that anharmonic electron-lattice interactions are essential for all transitions observed in the stripe phase of cuprates.

DOI: 10.1103/PhysRevB.92.024508 PACS number(s): 74.72.−h, 61.05.fm, 74.25.Kc, 74.62.Dh

Since the discovery of high-temperature superconductivity in $La_{2-x}Ba_xCuO_4$ (LBCO) [1], numerous intensive studies have revealed a complex interplay between charge, spin, orbital, and lattice degrees of freedom [2,3]. While the phase diagram of this cuprate family displays a generic complexity, a specific peculiarity is associated with it. In addition to the phase transition from the high-temperature tetragonal (HTT) phase with space group $I4/mmm$ to the low-temperature orthorhombic (LTO) phase ($Bmab$), a further transition takes place in LBCO from the LTO to a low-temperature tetragonal (LTT) phase ($P4_2/ncm$), which strongly depends on the Ba content x [4]. The phase transition from HTT to LTO occurs at $T_{LTO} \simeq 235$ K [5] and is accompanied by the tilting of the oxygen CuO_6 octahedra around the [110] direction, resulting in buckling distortions of all Cu-O-Cu bonds in the CuO_2 planes. At $T_{LTT} \simeq 55$ K, alternating octahedra tilt along [100] and [010] [5]. This restores the macroscopic fourfold symmetry, but it breaks the symmetry of the individual planes where half of the Cu-O-Cu bonds are buckled. The structural transition from LTO to LTT is accompanied by a prominent suppression of superconductivity that is largest for $x = 1/8$ [6]. This specific doping level is associated with static stripe order and linked to charge-spin-ordering [7–12]. The static charge order (CO) appears at the same temperature $T_{co} \simeq T_{LTT} \simeq 55$ K, and spin order (SO) sets in at $T_{so} \simeq 35$ K [5]. These results provide clear evidence for a subtle interplay between lattice, spin, and charge degrees of freedom. The experimental data indicate that unidirectional stripelike ordering is common to cuprates [13–15]. Despite various attempts [16–23], no consensus on the microscopic mechanism of stripe formation and the relevance of stripe correlations for high-temperature superconductivity in cuprates has been achieved.

The great interest in structural aspects of cuprates is related to the original idea leading to their discovery, namely Jahn-Teller polarons [1–3]. Substantial experimental evidence for a strong electron-lattice interaction has been reported for cuprates (see, e.g., [24,25]), including the unconventional oxygen isotope ($^{16}O/^{18}O$) effects (OIE's) on various quantities [24–30]. However, remarkable electronic properties of cuprates stimulated alternative proposals in terms of purely electronic pairing mechanisms (see, e.g., [19]). To explore the role of lattice dynamics on the various ordering temperatures in the stripe phase of cuprates, OIE studies [24–30] are essential.

A large OIE on the superconducting (SC) transition temperature T_c was reported for $La_{2-x}Ba_xCuO_4$ [31], $La_{1.6-x}Nd_{0.4}Sr_xCuO_4$ [32], and $La_{1.8-x}Eu_{0.2}Sr_xCuO_4$ [33] showing stripe order at $x = 1/8$ [34,35]. In addition, for $La_{2-x}Sr_xCuO_4$ ($x = 0.12, 0.15$) the OIE on the lattice parameters was investigated [31]. Moreover, for $La_{1.6-x}Nd_{0.4}Sr_xCuO_4$ a negative OIE on the structural phase-transition temperature T_{LTT} was detected by resistivity measurements [32]. Recently, we observed substantial OIE's on magnetic quantities characterizing the static spin-stripe order in $La_{2-x}Ba_xCuO_4$ with $x = 1/8$ (LBCO-1/8) [23]. However, no detailed OIE study of the structural properties and charge order in 1/8 doped cuprates has been undertaken.

In this paper, we report a negative OIE on T_{LTT} in LBCO-1/8 determined by means of high-resolution neutron powder diffraction with an OIE exponent $\alpha_{T_{LTT}} = -0.35(5)$, which has the same sign as $\alpha_{T_{so}} = -0.57(6)$ found for the spin-stripe order temperature T_{so} [23]. Since the LTT transition is accompanied by static charge order, we expect an OIE also to be present for the CO temperature. These results establish that all transitions observed in the stripe phase of LBCO-1/8 are sensitive to oxygen-ion-related lattice vibrations, indicating that these are relevant for stripe formation in the cuprates.

Polycrystalline samples of oxygen-substituted ($^{16}O/^{18}O$) $La_{2-x}Ba_xCuO_4$ with $x = 1/8$ were prepared in the same way as described in [23]. Magnetization, μSR, and powder neutron diffraction experiments were performed on samples from the same batch in order to study the OIE's on T_{c1} [23],

*zurab.guguchia@psi.ch

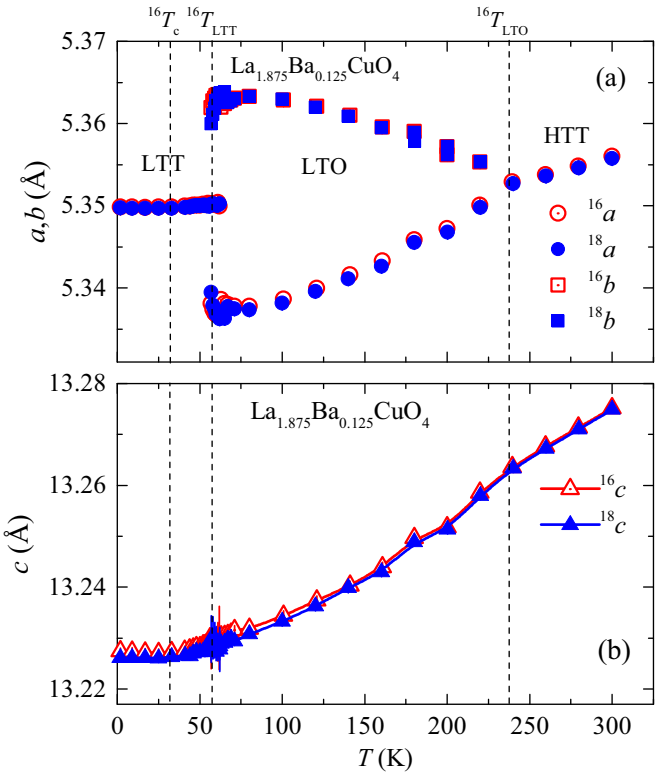

FIG. 1. (Color online) Temperature dependence of the lattice parameters a, b (a), and c (b) for the ^{16}O and ^{18}O samples of LBCO-1/8. The vertical lines mark the SC transition temperature $^{16}T_{c1}$ as well as the structural phase-transition temperatures $^{16}T_{LTT}$ and $^{16}T_{LTO}$.

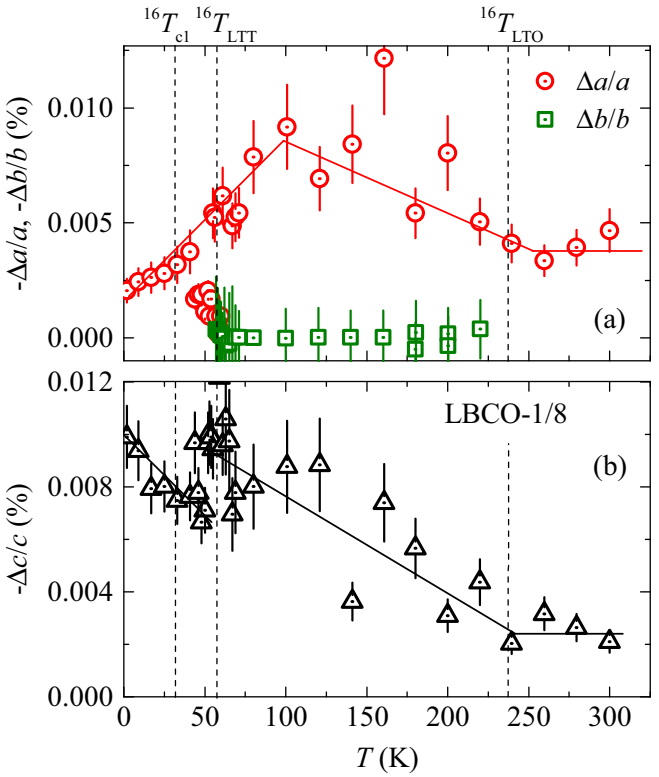

FIG. 2. (Color online) Temperature dependence of the relative oxygen isotope shifts $\Delta a/a$, $\Delta b/b$ (a), and $\Delta c/c$ (c) for the lattice parameters a, b, and c of LBCO-1/8. The vertical lines mark the SC transition temperature $^{16}T_{c1}$ as well as the structural phase-transition temperatures $^{16}T_{LTT}$ and $^{16}T_{LTO}$.

T_{so}, and T_{LTT} and to make a direct comparison between the OIE's on various quantities in the stripe phase of LBCO-1/8. The OIE exponents for T_{c1} and T_{so} are $\alpha_{T_c} = 0.46(6)$ and $\alpha_{T_{so}} = -0.56(9)$, respectively (see supplemental material [36] for details), being in perfect agreement with our previous results [23]. The neutron diffraction experiments were carried out at the high-resolution powder diffractometer HRPT [37] at the Swiss spallation neutron source SINQ at the Paul Scherrer Institut (PSI), Switzerland, with a wavelength of $\lambda = 1.494$ Å.

The OIE's on the LTT structural phase-transition temperature T_{LTT} and on the lattice parameters a, b, and c of LBCO-1/8 were studied by neutron diffraction. The average structure of LBCO-1/8 was assessed through Rietveld refinements to the raw diffraction data using the program FULLPROF [38] employing $I4/mmm$ (HTT), $Bmab$ (LTO), and $P4_2/ncm$ (LTT) models from the literature [5]. The crystal structure of LBCO-1/8 at room temperature (RT) was refined with the tetragonal $I4/mmm$ space group, and the corresponding lattice parameters are $a = 5.355(2)$ Å and $c = 13.275(7)$ Å at RT. The temperature dependence of the lattice parameters for the ^{16}O and ^{18}O samples of LBCO-1/8 are shown in Figs. 1(a) and 1(b). The LTO and LTT structural phase transitions are clearly visible in the temperature dependences of a and b. At $T_{LTO} \simeq 230$ K, a splitting of a and b reveals the transition to the LTO structure, which smoothly evolves from the HTT phase. Around $T_{LTT} \simeq 55$ K, these lattice parameters merge together, and a first-order transition from the LTO to the LTT phase takes place [4]. The c axis smoothly contracts with decreasing temperature [see Fig. 1(b)]. The values for T_{LTO} and T_{LTT} (marked by the vertical lines in Fig. 1) and those for the lattice parameters for the ^{16}O sample are in good agreement with published values [4,5]. The OIE's on the lattice constants are displayed in Figs. 2(a) and 2(b), where the temperature dependence of the relative isotope shifts of the lattice parameters $\Delta q/q = (^{18}q - ^{16}q)/^{16}q$ ($q = a, b, c$) are shown.

In all structural phases, the in-plane lattice parameter a for LBCO-1/8 decreases slightly upon replacing ^{16}O by ^{18}O. The quantity $\Delta a/a$ increases with decreasing temperature, reaching a maximum around $\simeq$100 K, and it decreases below. Interestingly, the lattice parameter b does not depend on oxygen isotope mass. The reason for this is not clear yet and requires further studies. At room temperature, $\Delta c/c$ is nearly the same as $\Delta a/a$. However, upon lowering the temperature, $\Delta c/c$ monotonically increases to become larger by a factor of 6 at the base temperature than at RT [39]. Reduction of all three lattice parameters with the heavier isotope was previously reported for $La_{2-x}Sr_xCuO_4$ ($x \sim 1/8$), however no temperature dependence of the isotope shifts was presented and discussed [31].

To illustrate the OIE on T_{LTT}, we plot the orthorhombic strain $\eta = 2(a-b)/(a+b)$ [5] for the two isotope samples as a function of temperature (see Fig. 3). η sharply drops to zero at $T_{LTT} \simeq 55$ K for the ^{16}O sample, consistent with the first-order

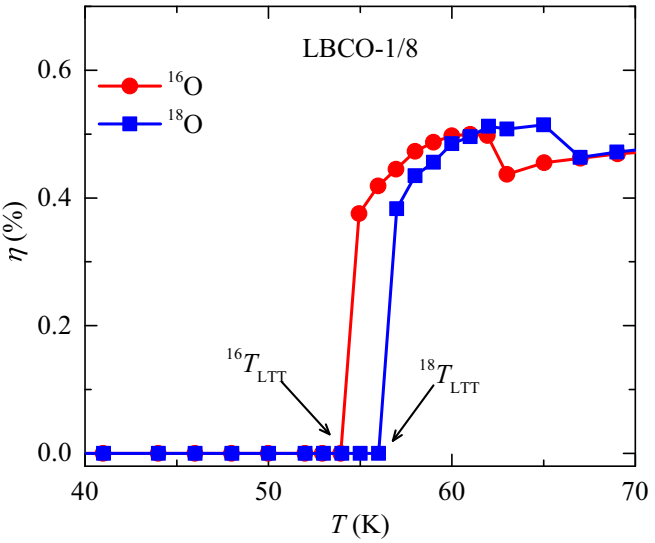

FIG. 3. (Color online) Temperature dependence of the orthorhombic strain $\eta = 2(a-b)/(a+b)$ for the ^{16}O and ^{18}O samples of LBCO-1/8. The arrows denote the LTT transition temperatures $^{16}T_{LTT}$ and $^{18}T_{LTT}$ for the ^{16}O and ^{18}O samples, respectively. The peculiarities at higher temperatures are artefacts connected with the exchange of the data treatment procedure.

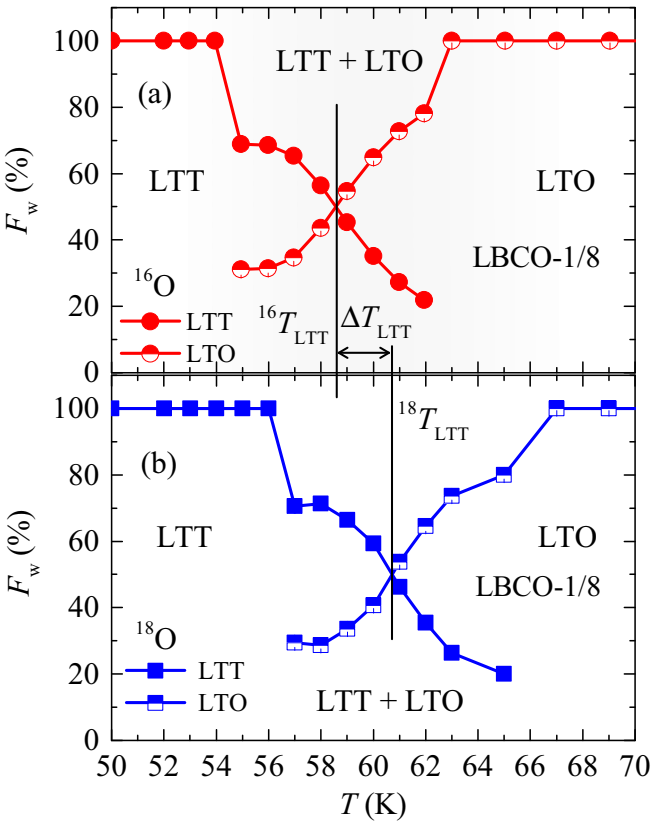

FIG. 4. (Color online) Temperature dependence of the relative weight fraction F_w of the LTT and LTO structural phases for the ^{16}O (a) and ^{18}O (b) samples of LBCO-1/8. The vertical lines mark the LTT transition temperatures $^{16}T_{LTT}$ and $^{18}T_{LTT}$ for the ^{16}O and ^{18}O samples, respectively.

nature of the LTT transition. The OIE on T_{LTT} is clearly visible as a pronounced shift to higher temperature with increasing isotope mass. The results for the OIE on T_{LTT} are $^{16}T_{LTT} = 54.5(3)$ K, $^{18}T_{LTT} = 56.5(3)$ K, and $\Delta T_{LTT} = {}^{18}T_{LTT} - {}^{16}T_{LTT} = 2.1(2)$ K, yielding an OIE exponent $\alpha_{T_{LTT}} = -0.36(5)$. This value is in good agreement with the previous value $\alpha_{T_{LTT}} \simeq -0.2$ for $La_{2-x}Nd_{0.4}Sr_xCuO_4$ ($x = 1/8$) extracted from resistivity measurements [32].

The detailed analysis of the diffraction patterns revealed that close to the structural transition, both the LTO and the LTT phase coexist over a temperature interval of $\simeq$8 K [40]. This is in line with the nature of the first-order structural phase transition at T_{LTT}, and it can be used as an alternative way to estimate the OIE on T_{LTT}. In Figs. 4(a) and 4(b), we plot the temperature dependences of the relative weight fractions F_w of the LTO and the LTT phase for the ^{16}O and ^{18}O samples, respectively. For the ^{16}O sample, the LTT phase appears below $\simeq$63 K, and F_w increases with decreasing temperature. The transition to the LTT phase is complete below 54 K, and between 54 and 63 K the LTT phase coexists with the LTO one. T_{LTT} is defined as the temperature where F_w of the LTO and the LTT phase are equal, yielding $^{16}T_{LTT} = 58.5(3)$ K, $^{18}T_{LTT} = 60.7(3)$ K, and $\alpha_{T_{LTT}} = -0.37(5)$, in excellent agreement with $\alpha_{T_{LTT}} = -0.36(5)$ obtained from the orthorhombic strain (Fig. 3). This demonstrates that the two independent methods for the determination of $\alpha_{T_{LTT}}$ yield consistent results.

The OIE on the structural phase-transition temperature T_{LTT} is accompanied by a clear shrinkage of the c axis with the heavier isotope in the temperature range from 2 to 300 K [see Fig. 2(b)]. Both phase transitions, i.e., the one from HTT to LTO and LTO to LTT, are accompanied by substantial phonon softening [4,41,42], where the first one is associated with the condensation of a degenerate pair of transverse-optic (TO) phonon modes at the X-point wave vector $q = (1/2,1/2,0)$, while the low-temperature one is driven by a soft Z-point phonon mode. This mode emerges from the high-temperature soft mode, which splits into two modes below T_{LTO}, corresponding to a zone-boundary mode at the (3,0,2) Z point and a zone-center one at the (0,3,2) Γ point. While the latter of the two modes hardens, the Z-point one continues to soften up to T_{LTT}. An understanding of this behavior and the transitional properties has been given in terms of a Landau free-energy expansion, where symmetry-invariant combinations of a degenerate order parameter Q_i ($i = 1,2$) and the orthorhombic strain η have been considered [4,43]:

$$F = 1/2\, a(T - T_0)\left(Q_1^2 + Q_2^2\right) + u\left(Q_1^2 + Q_2^2\right)^2 + v\left(Q_1^4 + Q_2^4\right) \cdots + c\eta^2/2 + d\left(Q_1^2 - Q_2^2\right)\eta + \cdots . \quad (1)$$

T_0 is the transition temperature, which depends on the coefficients a, u, v, c, and d, and it refers either to T_{HTT} or T_{LTT}. Within this approach, it is possible to construct the complex phase diagram, however isotope effects are absent. Clearly the observation of any kind of phase transition requires us to take into account strong lattice anharmonicity. This has already been emphasized in Ref. [44], in which the anomalous isotope effect on T_c as described in Ref. [31] was investigated. It was suggested that the structural instability is driven by

anharmonicity, which in turn affects the electronic density of states. Thereby, a large isotope effect on T_c is possible that exceeds the conventional BCS one. In this approach, however, no isotope effect on the structural transition has been considered. These are obtained within a dynamic anharmonic electron lattice interaction Hamiltonian, which reduces in the limit in which only the soft modes are taken into account, to [3]

$$H = \sum_i \frac{p_i^2}{2m} - \frac{g_2}{2} W_i^2 + \frac{g_4}{4} W_i^4 + \sum_{i,f} f(W_i - W_j)^2 + \cdots , \tag{2}$$

with p_i being the momenta in cell i, m is the oxygen ion mass, g_2, g_4 are the harmonic and fourth-order electron-ion interaction constants, W_i is the relative electron-ion displacement coordinate, and f is the long-range interaction between sites i and j. The fourth-order term proportional to g_4 is treated within the self-consistent phonon approximation (SPA). Within the SPA, this corresponds to a cumulant expansion of the nonlinear term in the displacement-displacement correlation function by means of which a temperature dependence in the phonon frequencies is introduced:

$$\begin{aligned} g_T &= g_2 + 3g_4\langle W^2\rangle_T \\ &= g_2 + 3g_4 \sum_{i,q} \frac{\hbar}{m\omega(i,q)} W^2(i,q) \coth\frac{\hbar\omega}{2kT}. \end{aligned} \tag{3}$$

The sum is over all phonon branches i and momenta q with phonon frequency $\omega(i,q)$ and contains all dynamical information. A phase transition takes place if $g_T = 0$ for a given q value. While Eq. (3) does not admit an analytical solution, an approximate formula for T_0 has been given in Ref. [45]:

$$T_0 = \hbar g_4 \sqrt{f}\left[g_2^2\sqrt{m}\,\mathrm{arccoth}\{2\sqrt{fm}g_2/(3g_4\hbar)\}\right]^{-1}. \tag{4}$$

To determine the correct symmetry of the soft mode, the free energy [Eq. (1)] has to be employed for the corresponding order parameter. This is included in Eq. (2) by solving the equations of motion and taking the zero solution for the soft mode at the appropriate q value from which T_0 is also obtained. A simplified solution of T_0 is given by Eq. (3), from which an isotope effect on T_0 is derived with the parameter values of Ref. [3] for g_2, g_4, and f as appropriate for the $x = 1/8$ doping, yielding $^{16}T_0 \simeq 54.8$ K and $^{18}T_0 \simeq 57.0$ K. This corresponds to an OIE exponent of $\alpha_{T_0} \simeq -0.39$, in good agreement with the experimental value $\alpha_{T_{\rm LTT}} = -0.36(5)$. Importantly, the calculated values for $^{16}T_0$ and $^{18}T_0$ are consistent with the experimental values $^{16}T_{\rm LTT}$ and $^{18}T_{\rm LTT}$ given above. The Z-point related soft phonon mode is derived within the SPA from the equations of motion for the two isotopes. Figure 5(a) shows the calculated temperature dependence of the Z-point related phonon mode frequency ω_Z. In this case, the transition temperatures are $^{16}T_0 \simeq 52.1$ K and $^{18}T_0 \simeq 54.8$ K, which are slightly shifted to lower temperatures as compared to the experimental values. However, the corresponding OIE exponent $\alpha_{T_0} \simeq -0.49$ is in agreement with the experiment. To achieve an additional correspondence between experiment and theory, the relative mean-square Cu-O displacement δx along the c axis is calculated for both isotopes, ^{16}O and ^{18}O, respectively, and their relative difference $\Delta(\delta x)/\delta x = (^{18}\delta x - ^{16}\delta x)/^{16}\delta x$ is shown in Fig. 5(b). The relative displacement for ^{18}O is smaller than for ^{16}O, in agreement with the data for the lattice parameter c. In Fig. 5(b), the temperature dependence of the relative isotope shift $\Delta(\delta x)/\delta x$ is shown together with $\Delta c/c$ taken from Fig. 2(b). While a temperature-independent systematic shift in absolute values is visible, there is salient agreement in the corresponding temperature dependences, providing strong evidence that the LTT structural phase transition is driven by phonon mode softening caused by anharmonic electron-lattice interactions [46–50].

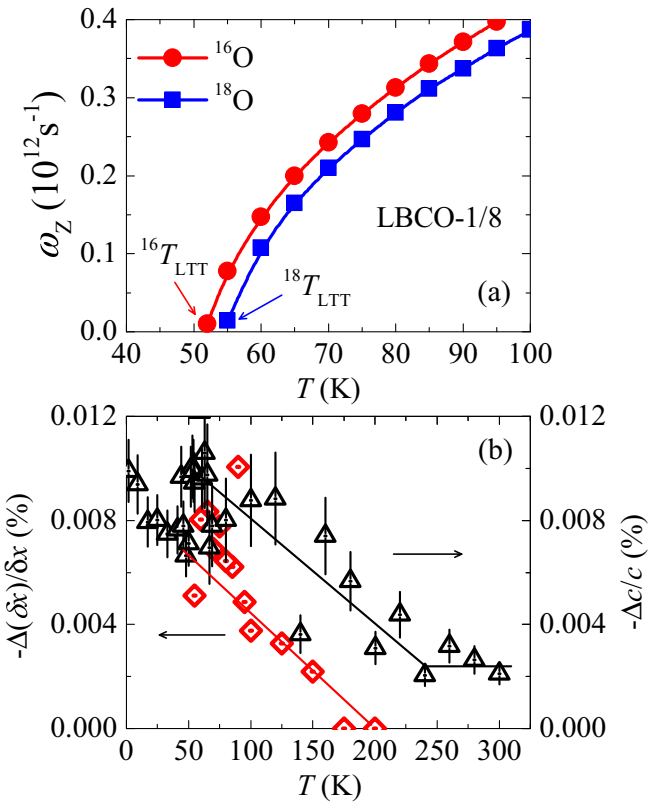

FIG. 5. (Color online) Calculated temperature dependence of the Z-point related phonon mode frequency ω_Z (a) and the relative isotope shift of the dynamical relative oxygen-copper displacement $\Delta(\delta x)/\delta x$ (b) of LBCO-1/8, plotted together with $\Delta c/c$, taken from Fig. 2(b).

In conclusion, oxygen isotope effects on lattice properties in the static stripe phase of LBCO-1/8 were investigated by means of neutron diffraction. The low-temperature tetragonal phase-transition temperature $T_{\rm LTT}$ exhibits a large negative OIE with $\alpha_{T_{\rm LTT}} = -0.36(5)$. In addition, the temperature-dependent contraction of the c axis with the heavier isotope is observed. Since the LTT transition is linked to static charge order, we expect an OIE to be present for the CO temperature as well. These results combined with the previously observed OIE on $T_{\rm so}$ show that all transitions observed in the stripe phase of LBCO-1/8 are sensitive to oxygen lattice vibrations. The theoretical lattice-dynamical calculations based on a dynamic anharmonic electron lattice interaction Hamiltonian consistently reproduce the experimental results. This structural instability is driven by phonon mode softening stemming from anharmonic electron-lattice interactions, which are essential for the stripe formation in the cuprates.

We acknowledge Elvezio Morenzoni, Vladimir Pomjakushin, and Jonathan White for helpful discussions. This work was supported by the Swiss National Science Foundation, the NCCR MaNEP, the SCOPES Grant No. IZ74Z0-137322, and the Georgian National Science Foundation Grant No. RNSF/AR/10-16. This work is partly based on experiments performed at the Swiss spallation neutron source SINQ, Paul Scherrer Institute, Villigen, Switzerland.

[1] J. G. Bednorz and K. A. Müller, Z. Phys. B **64**, 189 (1986).
[2] J. D. Jorgensen, H. B. Schuttler, D. G. Hinks, D. W. Capone, K. Zhang, M. B. Brodsky, and D. J. Scalapino, Phys. Rev. Lett. **58**, 1024 (1987).
[3] A. Bussmann-Holder, A. Migliori, Z. Fisk, J. L. Sarrao, R. G. Leisure, and S.-W. Cheong, Phys. Rev. Lett. **67**, 512 (1991).
[4] J. D. Axe, A. H. Moudden, D. Hohlwein, D. E. Cox, K. M. Mohanty, A. R. Moodenbaugh, and Y. Xu, Phys. Rev. Lett. **62**, 2751 (1989).
[5] M. Hücker, M. V. Zimmermann, G. D. Gu, Z. J. Xu, J. S. Wen, G. Xu, H. J. Kang, A. Zheludev, and J. M. Tranquada, Phys. Rev. B **83**, 104506 (2011).
[6] A. R. Moodenbaugh, Y. Xu, M. Suenaga, T. J. Folkerts, and R. N. Shelton, Phys. Rev. B **38**, 4596 (1988).
[7] G. M. Luke, L. P. Le, B. J. Sternlieb, W. D. Wu, Y. J. Uemura, J. H. Brewer, T. M. Riseman, S. Ishibashi, and S. Uchida, Physica C **185-189**, 1175 (1991).
[8] M. K. Crawford, M. Kunchur, W. E. Farneth, E. M. McCarron, and S. J. Poon, Physica C **162–164**, 755 (1989).
[9] J. M. Tranquada, B. J. Sternlieb, J. D. Axe, Y. Nakamura, and S. Uchida, Nature (London) **375**, 561 (1995).
[10] J. M. Tranquada, J. D. Axe, N. Ichikawa, Y. Nakamura, S. Uchida, and B. Nachumi, Phys. Rev. B **54**, 7489 (1996).
[11] P. Abbamonte, A. Rusydi, S. Smadici, G. D. Gu, G. A. Sawatzky, and D. L. Feng, Nat. Phys. **1**, 155 (2005).
[12] M. Hücker, M. V. Zimmermann, M. Debessai, J. S. Schilling, J. M. Tranquada, and G. D. Gu, Phys. Rev. Lett. **104**, 057004 (2010).
[13] S. A. Kivelson, I. P. Bindloss, E. Fradkin, V. Oganesyan, J. M. Tranquada, A. Kapitulnik, and C. Howald, Rev. Mod. Phys. **75**, 1201 (2003).
[14] M. Vojta, Adv. Phys. **58**, 699 (2009).
[15] Y. Kohsaka, C. Taylor, K. Fujita, A. Schmidt, C. Lupien, T. Hanaguri, M. Azuma, M. Takano, H. Eisaki, H. Takagi, S. Uchida, and J. C. Davis, Science **315**, 1380 (2007).
[16] J. M. Tranquada, G. D. Gu, M. Hücker, Q. Jie, H.-J. Kang, R. Klingeler, Q. Li, N. Tristan, J. S. Wen, G. Y. Xu, Z. J. Xu, J. Zhou, and M. V. Zimmermann, Phys. Rev. B **78**, 174529 (2008).
[17] T. Valla, A. V. Federov, J. Lee, J. C. Davis, and G. D. Gu, Science **314**, 1914 (2006).
[18] Q. Li, M. Hücker, G. D. Gu, A. M. Tsvelik, and J. M. Tranquada, Phys. Rev. Lett. **99**, 067001 (2007).
[19] E. Berg, E. Fradkin, E.-A. Kim, S. A. Kivelson, V. Oganesyan, J. M. Tranquada, and S. C. Zhang, Phys. Rev. Lett. **99**, 127003 (2007).
[20] R.-H. He, K. Tanaka, S.-K. Mo, T. Sasagawa, M. Fujita, T. Adachi, N. Mannella, K. Yamada, Y. Koike, Z. Hussain, and Z.-X. Shen, Nat. Phys. **5**, 119 (2009).
[21] J. M. Tranquada, AIP Conf. Proc. **1550**, 114 (2013).
[22] Z. Guguchia, A. Maisuradze, G. Ghambashidze, R. Khasanov, A. Shengelaya, and H. Keller, New J. Phys. **15**, 093005 (2013).
[23] Z. Guguchia, R. Khasanov, M. Bendele, E. Pomjakushina, K. Conder, A. Shengelaya, and H. Keller, Phys. Rev. Lett. **113**, 057002 (2014).
[24] K. A. Müller, J. Phys.: Condens. Matter **19**, 251002 (2007).
[25] H. Keller, A. Bussmann-Holder, and K. A. Müller, Mater. Today **11**, 9 (2008); H. Keller and A. Bussmann-Holder, Adv. Condens. Matter Phys. **2010**, 393526 (2010).
[26] A. Shengelaya, G.-m. Zhao, C. M. Aegerter, K. Conder, I. M. Savić, and H. Keller, Phys. Rev. Lett. **83**, 5142 (1999).
[27] R. Khasanov, A. Shengelaya, D. Di Castro, E. Morenzoni, A. Maisuradze, I. M. Savić, K. Conder, E. Pomjakushina, A. Bussmann-Holder, and H. Keller, Phys. Rev. Lett. **101**, 077001 (2008).
[28] A. Lanzara, G.-m. Zhao, N. L. Saini, A. Bianconi, K. Conder, H. Keller, and K. A. Müller, J. Phys.: Condens. Matter **11**, L541 (1999).
[29] D. Rubio Temprano, J. Mesot, S. Janssen, A. Furrer, K. Conder, and H. Mutka, Phys. Rev. Lett. **84**, 1990 (2000).
[30] P. S. Häfliger, S. Gerber, R. Pramod, V. I. Schnells, B. dalla Piazza, R. Chati, V. Pomjakushin, K. Conder, E. Pomjakushina, L. Le Dreau, N. B. Christensen, O. F. Syljuåsen, B. Normand, and H. M. Rønnow, Phys. Rev. B **89**, 085113 (2014).
[31] M. K. Crawford, W. E. Farneth, E. M. McCarronn III, R. L. Harlow, and A. H. Moudden, Science **250**, 1390 (1990).
[32] G. Y. Wang, J. D. Zhang, R. L. Yang, and X. H. Chen, Phys. Rev. B **75**, 212503 (2007).
[33] Suryadijaya, T. Sasagawa, and H. Takagi, Physica C **426**, 402 (2005).
[34] M. K. Crawford, R. L. Harlow, E. M. McCarron, W. E. Farneth, J. D. Axe, H. Chou, and Q. Huang, Phys. Rev. B **44**, 7749 (1991).
[35] B. Büchner, M. Breuer, A. Freimuth, and A. P. Kampf, Phys. Rev. Lett. **73**, 1841 (1994).
[36] See Supplemental Material at http://link.aps.org/supplemental/10.1103/PhysRevB.92.024508 for details on the OIE exponents.
[37] P. Fischer, G. Frey, M. Koch, M. Konnecke, V. Pomjakushin, J. Schefer, R. Thut, N. Schlumpf, R. Burge, U. Greuter, S. Bondt, and E. Berruyer, Physica B **276–278**, 146 (2000).
[38] J. Rodríguez-Carvajal, Physica B **192**, 55 (1993).
[39] Note that some peculiar features close to T_{LTT} are visible. However, due to the fact that close to the LTT-to-LTO structural phase transition both phases coexist (see the discussion below), these peculiarities are likely related to artefacts caused by the exchange of the data treatment procedure.
[40] Since F_w becomes temperature-dependent close to the transition, the data in Fig. 3 are plotted down to the temperatures at which a well-refineable orthorhombic phase was present.
[41] H. Kimura, Y. Noda, H. Goka, M. Fujita, K. Yamada, and G. Shirane, J. Phys.: Soc. Jpn. **74**, 445 (2005).
[42] B. Keimer, R. J. Birgenau, A. Cassanho, Y. Endoh, M. Greven, M. A. Kastner, and G. Shirane, Z. Phys. B **91**, 373 (1993).
[43] W. Ting, K. Fossheim, and T. Laegreid, Solid State Commun. **75**, 727 (1990).

[44] W. E. Pickett, R. E. Cohen, and H. Krakauer, Phys. Rev. Lett. **67**, 228 (1991).
[45] A. Bussmann-Holder, J. Phys.: Condens. Matter **24**, 273202 (2012).
[46] A. Bussmann-Holder, A. Simon, and A. R. Bishop, Z. Kristallogr. **226**, 177 (2011).
[47] G. Mahan, Phys. Rev. B **56**, 8322 (1997).
[48] J. Zhong and H.-B. Schüttler, Phys. Rev. Lett. **69**, 1600 (1992).
[49] A. Bussmann-Holder and A. R. Bishop, Phys. Rev. B **44**, 2853 (1991).
[50] J. E. Hirsch, Phys. Rev. B **47**, 5351 (1993).